Hydrogen Atom Abstraction from CH 4 by Nanosized Vanadium Oxide Cluster Cations

ARTICLE *in* THE JOURNAL OF PHYSICAL CHEMISTRY C · OCTOBER 2014

Impact Factor: 4.77 · DOI: 10.1021/jp5059403

5 AUTHORS, INCLUDING:

Wu Xiao-Nan
Technische Universität Berlin
43 PUBLICATIONS **896** CITATIONS
SEE PROFILE

Xun-Lei Ding
North China Electric Power University
57 PUBLICATIONS **1,592** CITATIONS
SEE PROFILE

Yan-Xia Zhao
Chinese Academy of Sciences
40 PUBLICATIONS **926** CITATIONS
SEE PROFILE

Sheng-Gui He
Chinese Academy of Sciences
153 PUBLICATIONS **2,458** CITATIONS
SEE PROFILE

THE JOURNAL OF PHYSICAL CHEMISTRY C

Article

pubs.acs.org/JPCC

Hydrogen Atom Abstraction from CH_4 by Nanosized Vanadium Oxide Cluster Cations

Xiao-Nan Wu,[†] Xun-Lei Ding,*[,‡] Zi-Yu Li,[†] Yan-Xia Zhao,*[,†] and Sheng-Gui He[†]

[†]Beijing National Laboratory for Molecular Science, State Key Laboratory for Structural Chemistry of Unstable and Stable Species, Institute of Chemistry, Chinese Academy of Sciences, Beijing, 100190, P. R. China

[‡]Department of Mathematics and Physics, North China Electric Power University, Beinong Road 2, Huilongguan, Beijing, 102206, P. R. China

Supporting Information

ABSTRACT: Reactions of vanadium oxide cluster cations with methane in a fast-flow reactor were investigated with a time-of-flight mass spectrometer. Hydrogen atom abstraction (HAA) reactions were identified over stoichiometric cluster cations $(V_2O_5)_N^+$ for N as large as 11, and the relative reactivity decreases as the cluster size increases. Density functional calculations were performed to study the structural, bonding, and electronic properties of the stoichiometric oxide clusters with the size N = 2−6. The geometric structures were obtained by means of topological and structural unit analyses together with global optimizations. Two types of oxygen-centered radicals were found in these clusters, which are active sites of the clusters in reactions with CH_4. The size-dependent reactivity is rationalized by the charge, spin, and structural effects. This work is among the first reports that HAA from CH_4 can take place on *nanosized* oxide clusters, which makes a bridge between the small reactive species and inert condensed phase materials for CH_4 activation under low temperature.

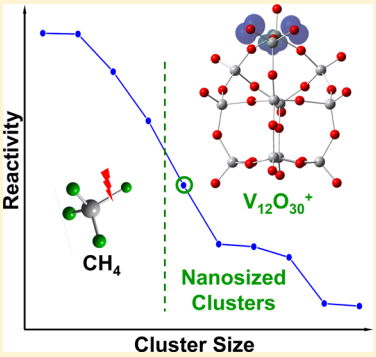

1. INTRODUCTION

Methane (CH_4), as the principal component of natural gas, is considered as a potential feedstock to replace dwindling petroleum for the synthesis of value-added products.[1−3] However, the conversion of CH_4 is really a challenge because of strong C−H bonds and low reactivity of CH_4.[4,5] High temperature is always necessary in the reactions on the surface of traditional metal or metal oxide catalysts, and as a consequence, undesirable pathways such as overoxidation are hard to avoid.[6−8] In the activation of CH_4, hydrogen atom abstraction (HAA) from CH_4 to produce $CH_3^•$ radical is considered to be the decisive step in the oxidative dehydrogenation and dimerization of CH_4.[9−12] However, the reaction mechanisms of HAA are not yet very clear.

Gas-phase atomic clusters may serve as ideal models to study reaction mechanisms at a molecular level, because they can be examined under isolated, controlled, and reproducible conditions in experiments and reliably handled by theoretical quantum chemical calculations.[13] Various gas-phase species have been found to be able to abstract one H atom from CH_4 at near room temperature.[14−17] They include not only some atomic[18] or polyatomic metal ions[19] and ligated metal clusters,[20] but also many oxide cluster cations, such as transition metal oxides OsO_4^+,[21] FeO^+,[22] MnO^+,[23] MoO_3^+,[24] TiO_2^+, ZrO_2^+,[25] $V_4O_{10}^+$,[26] $(TiO_2)_{1-5}^+$, $(ZrO_2)_{1-4}^+$, $(HfO_2)_{1-2}^+$, $(V_2O_5)_{1-5}^+$, $(Nb_2O_5)_{1-3}^+$, $(Ta_2O_5)_{1-2}^+$, $(MoO_3)_{1-2}^+$, $(WO_3)_{1-3}^+$, $Re_2O_7^+$,[27] and $(CeO_2)_{2-4}^+$;[28] main group metal oxides MgO^+,[29] $(Al_2O_3)_{3-5}^+$,[30,31] CaO^+, SrO^+, BaO^+,[32] PbO^+,[33] SnO^+, GeO^+;[34] metal-free oxides SO_2^+,[35] $P_4O_{10}^+$,[36] CO^+, and SiO^+;[37] as well as heteronuclear oxide clusters $AlVO_4^+$,[38] $V_2O_5(SiO_2)_{1-4}^+$, $(V_2O_5)_2SiO_2^+$,[39] $V_{4-n}P_nO_{10}^+$ (n = 1, 2),[40,41] $V_{4-n}Y_nO_{10}^+$ (n = 1, 2),[42] $AlYO_3^+$,[43] and $NbAuO_3^+$.[44] Oxygen-centered radicals ($O^{•-}$) were found in most of these clusters which were suggested as the active site for HAA.[16,17,45,46] Note that HAA can also take place on free $O^{•-}$ radicals,[47] but the detailed reaction mechanisms on free and ligated $O^{•-}$ over atomic clusters are different.[46]

Though fruitful results have been achieved in the above-mentioned gas-phase studies, it should be pointed out that reactive clusters found in the experiments are all of small size, typically with 1−5 metal atoms. The largest ones may be $Al_{10}O_{15}^+$ and $V_{10}O_{25}^+$,[27,31] whose diameters are still below 1 nm.[48,49] An important question may be raised by researchers of cluster science as well as practical catalysis: whether or not the chemistry of the studied small clusters is really applicable for interpreting the reactions taking place on catalyst surfaces. It seems that there exists a big gap between the subnanosized reactive species on which HAA from CH_4 may take place and the condensed phase surfaces which are usually inert toward CH_4 under low temperature. To narrow this gap, a "bottom up" approach is to study various properties of the reactive clusters and especially the size-dependent reactivity of clusters with size up to nanoscale. Our recent work found that large-sized scandium oxide clusters, such as $Sc_{44}O_{66}^+$ (~1.36 nm), are able to abstract one H atom

Received: June 15, 2014
Revised: August 23, 2014
Published: September 22, 2014

from more reactive alkanes (such as C_4H_{10}) but not CH_4.[50] This indicates that nanosized oxide clusters may still have high reactivity toward C−H activation, and researchers are hopeful to find one that can activate CH_4.

In this work, we studied large sized vanadium(V) oxide clusters to investigate the possibility of CH_4 activation on nanosized oxide clusters, and achieved encouraging results. We selected V because $V_4O_{10}^+$ is the first reported polynuclear oxide clusters on which HAA may take place[26] while $V_{10}O_{25}^+$ is the largest one so far,[27] and supported vanadia species (such as on V_2O_5/SiO_2) have been widely used and extensively studied for partial oxidation of CH_4 to synthesis gas, methanol, or formaldehyde.[51−56]

2. EXPERIMENTAL DETAILS AND COMPUTATIONAL METHODS

A reflectron time-of-flight mass spectrometer (TOF-MS) coupled with a laser ablation/supersonic expansion cluster source and a fast flow reactor was used in the experiments (see ref 50 for details). Metal oxide clusters were generated by laser ablation of V metal disk in the presence of O_2 (2%) seeded carrier gas (He), controlled by a pulsed valve. Then the generated clusters were expanded to the reactor, where they reacted with the reactant gases (CH_4 or CD_4 diluted in the buffer gas He) controlled by the second pulsed valve. The instantaneous total gas pressure in the reactor was estimated to be around 220 Pa at 300 K.[57] After multiple collisions with the carrier gas and the buffer gas before reacting with CH_4 or CD_4, the cluster vibrational temperature in the reactor was estimated to be close to 300−350 K in our recent experiments.[58] Considering that the absolute reaction rate of $V_4O_{10}^+$ with CH_4 determined in our experiment[27] is lower by a factor of 5 than that obtained by Feyel and co-workers[26] using a VG BIO-Q mass spectrometer of QHQ configuration (Q, quadrupole; H, hexapole) equipped with an electrospray ionization (ESI) source, the temperature of clusters in our experiments is no higher than that in theirs, which was stated at near room temperature. To prevent residual water in the gas handling system leading to undesirable hydroxo species, the prepared gas mixture (O_2/He) and reactant gases were passed through long copper tube coils at low temperatures (77 K and 190−240 K, respectively) before they entered the pulsed valves. The reflectron TOF-MS was used to measure the cluster abundances before and after the reactions. The mass resolution of the TOF-MS is approximately 3000 ($M/\Delta M$) with the current experimental setup, and the uncertainty of the reported relative ion signals is about 10%.

Density functional theory (DFT) calculations with the hybrid B3LYP functional[59−61] and the Gaussian 09 program[62] were performed to study the geometric and electronic structures of $(V_2O_5)_N^+$ clusters for N = 2−6. It has been demonstrated that B3LYP is able to give reasonably good results for V oxide clusters compared with various experiments such as infrared (multiple-photon) photodissociation (IRPD/IRMPD),[63−66] collision-induced dissociation (CID),[67−69] and photoelectron spectroscopy (PES).[70] The polynuclear metal oxide clusters can have a high number of possible stable structures. A Fortran code based on a genetic algorithm (GA) was developed and has successfully been applied on lanthanum oxide clusters.[71] Such a code was used to generate initial guess structures with small basis sets (LANL2DZ)[72−74] and coarse convergence thresholds in both self-consistent field and optimization steps to reduce the computational costs. Then more than 20 low-lying isomers for each cluster were reoptimized with larger basis sets, in which all-electron basis sets with triple-ζ valence and polarization (TZVP)[75] were used. Vibrational frequency calculations with the same basis sets have been performed to check that all stable structures have no imaginary frequency, and the calculated energies reported here are all with zero-point vibrational energy correction unless specified.

3. RESULTS

3.1. Experimental Mass Spectra for HAA. Selected TOF mass spectra for interactions of $V_xO_y^+$ with CH_4 (and CD_4) in the reactor are shown in Figure 1 (see Figure S1 in the Supporting Information for complete spectra). Upon the interaction with CH_4 in the reactor (panels b1 and b2), the signal magnitudes of $V_{12}O_{30}^+$ and $V_{14}O_{35}^+$ decrease significantly, while those of the one more oxygen-rich clusters (i.e., $V_{12}O_{31}^+$ and $V_{14}O_{36}^+$) do not change within the experimental uncertainties. Meanwhile, products that can be assigned as $V_{12}O_{30}H^+$ and $V_{14}O_{35}H^+$ appear. Further increase of the CH_4 partial pressure in the reactor generates more intense signals of the products (panels c1 and c2). This indicates that HAA reactions take place on the stoichiometric cluster cations $(V_2O_5)_N^+$ (N = 6 and 7), which is further supported by the isotopic labeling experiment (panels d1 and d2). In panels b3 and b4, we present the spectra for the reactions of CH_4 on $V_{20}O_{50}^+$ and $V_{22}O_{55}^+$ (i.e., N = 10 and 11) as examples for the HAA on large clusters. In a summary, HAA channel is found in the following reactions:

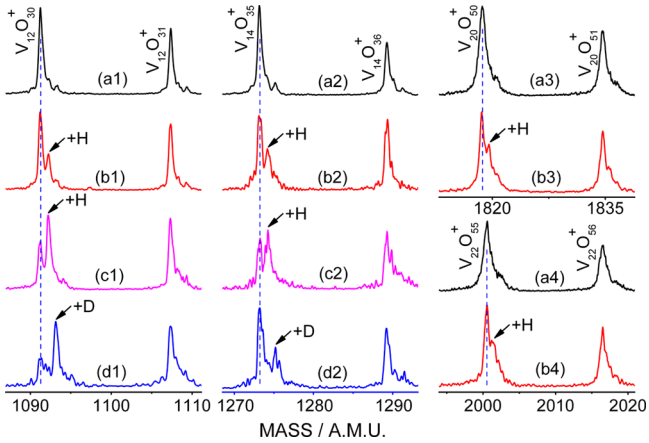

Figure 1. Selected time-of-flight mass spectra for the generation and reaction of $V_xO_y^+$ clusters with He gas for reference (a), CH_4 (b and c), and CD_4 (d). Pressures are 7.8 (23.7), 26.1 (49.7), 35.5, and 35.5 Pa for CH_4 in b1−4 (c1 and c2 in parentheses), respectively, and 34.7 Pa for CD_4. Signals of stoichiometric clusters $(V_2O_5)_N^+$ (N = 6, 7, 10, and 11) are indicated by dashed lines, and those for the corresponding products are labeled with +H or +D.

$$(V_2O_5)_N^+ + CH_4 \rightarrow (V_2O_5)_NH^+ + CH_3 \quad (N = 2 - 11) \tag{1}$$

Reactions for even larger clusters (N > 11) are not very evident in our experiments due to the relatively low resolution and low reactivity. The estimated diameters of $(V_2O_5)_N$ clusters may exceed 1 nm when $N \geq 6$, so all the V oxide clusters shown in Figure 1 can be taken as *nanosized* clusters.[76] Note that HAA reactions on subnanosized clusters $(V_2O_5)_{1-5}^+$ have been observed in previous works.[26,27]

3.2. Experimental Rate Constants for HAA. The pseudo-first-order rate constants (k_1) for depletion of $(V_2O_5)_N^+$ by CH_4 and CD_4 were calculated by

dx.doi.org/10.1021/jp5059403 | J. Phys. Chem. C 2014, 118, 24062−24071

$$k_1 = \ln(I_0/I)/(\rho\Delta t) \quad (2)$$

in which I_0 and I are signal magnitudes of $(V_2O_5)_N^+$ in the absence and presence of reactant gas, respectively; ρ is the molecular density of reactant gas density;[57] and Δt is the reaction time ($\Delta t = l/v$, in which $l \approx 60$ mm is the reactor length and $v \approx 1$ km/s is the cluster beam velocity). The absolute values of k_1 may be systematically under- or overestimated due to systematic deviation in determining the values of ρ and Δt in the pulse experiment, while the deviation is within a factor of 5 by comparing the rate constants from our fast flow reaction experiments with those from other independent experiments.[39] For example, the absolute value of $k_1(V_4O_{10}^+ + CH_4)$ is 1.3×10^{-10} or 5.5×10^{-10} cm^3 molecule^{-1} s^{-1} determined by using our fast flow reaction experiment[27] or the QHQ experiment,[26] respectively. To compare the relative reactivity of the reactive clusters $(V_2O_5)_N^+$ (N = 2−11), relative rate constants with respect to $k_1(V_4O_{10}^+ + CH_4)$, denoted as k_1^{rel}, were calculated and shown in Figure 2. The uncertainty of k_1^{rel} is expected to be near

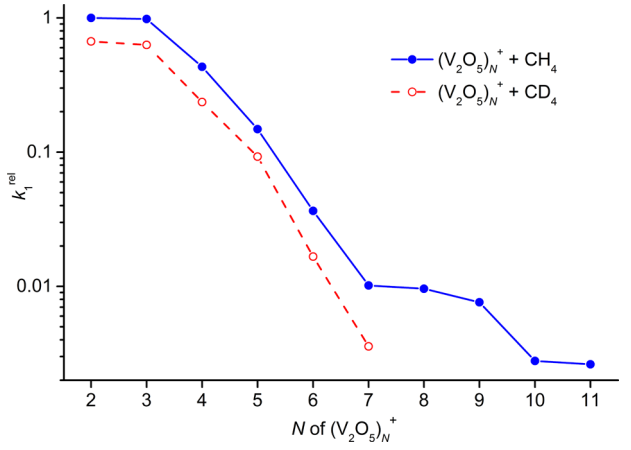

Figure 2. Relative rate constants (k_1^{rel}) of the reactions of $(V_2O_5)_N^+$ clusters with either CH_4 or CD_4.

20%.[39] The reactivity with CD_4 shows trends consistent with that of CH_4. Kinetic isotope effect (KIE) values are estimated to be around 1.5−2.8, and larger KIE values correspond to the reaction systems with relatively lower reactivity. In the following, we discuss with CH_4 unless specified.

Generally, k_1^{rel} decreases monotonically when N increases from 2 to 11 for reactions with CH_4, and $(V_2O_5)_{11}^+$ has the smallest value of k_1^{rel} as 2.6×10^{-3}. The estimated absolute rate constant k_1 ranges from 1.3×10^{-10} cm^3 molecule^{-1} s^{-1} for $V_4O_{10}^+$ to 3.4×10^{-13} cm^3 molecule^{-1} s^{-1} for $(V_2O_5)_{11}^+$, and the reaction efficiencies Φ (= k_1/k_{CR}, in which k_{CR} is the collision rate) range from 0.16 to 2×10^{-4}.[77] It is clear that although all of the clusters $(V_2O_5)_N^+$ (N = 2−11) can abstract H atom from methane, their relative reactivity differs largely, by 3 orders of magnitude. It is interesting to find that k_1^{rel} decreases rapidly before N = 7 (except from N = 2 to N = 3) and quite gently after that, indicating that HAA may also take place on $(V_2O_5)_N^+$ of even larger size.

3.3. Calculated Structures of $(V_2O_5)_N^+$ and $(V_2O_5)_N$ Clusters. For verification of the high reactivity toward CH_4 and attainment of additional structure−property relationship of $(V_2O_5)_N^+$ clusters, it is essential to determine the structure of each cluster at first. Due to excessive computational cost for large clusters, we studied only the clusters with $N \leq 6$, for which the relative reactivity changes rapidly. As a starting point and also for comparison, low-lying structures of neutral clusters were also studied.

Figure 3 shows the calculated most stable structures for neutral $(V_2O_5)_N$ (N = 2−6) clusters, denoted as $\mathbf{V_{2N}\_1}$, in which 2N is

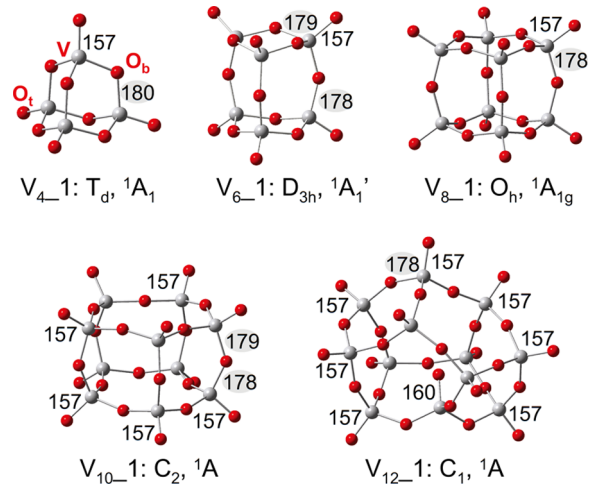

Figure 3. DFT optimized most stable structure for each of the neutral $(V_2O_5)_N$ (N = 2−6) clusters. The symmetry and electronic state are listed below each structure. Some bond lengths between V and terminal or bridging bonded O atoms (O_t or O_b) are given in pm.

the number of V atoms, and more isomeric structures ($\mathbf{V_{2N}\_1}$−**6**) are provided in Supporting Information Figure S2. Most of these structures (all in Figure 3 and most of those in Supporting Information Figure S2) are constructed by the same structural unit, $V(O_b)_3O_t$, in which each V is coordinated with three bridging bonded O atoms (denoted as O_b) and one terminal bonded O atom (O_t). These structures can be viewed as polyhedron structure (V atoms are the vertices and each V−O_b−V forms an edge) when all the O_t atoms are ignored. Each vertex has 3 edges in these polyhedrons (just like fullerenes), so the topological structures are three-dimensional 3-regular graphs, which can be generated by a modified code of CaGe.[78] The polyhedron structure with k of g-edge polygons as the surfaces is denoted as $P(g^k)$. For example, the structures in Figure 3 are $P3^4$, $P3^24^3$, $P4^6$, $P4^55^2$, and $P4^45^4$, respectively. In the calculations g is limited as $3 \leq g \leq 6$ (i.e., the surfaces of the polyhedron are restricted to be trigon, tetragon, pentagon, or hexagon), since test calculations indicate that structures with $g > 6$ are all with high relative energies. As the cluster size increases, the number of isomeric polyhedron structures increases very quickly: 1 for N = 2 and 3; and 2, 5, and 10 for N = 4−6, respectively. Calculations on these polyhedron structures indicate that those with only g = 4 and 5 are preferred for both neutral and cationic clusters. These polyhedron structures were used as a part of initial structures for GA optimizations, and they are found to be much more favorable than other structures for neutral clusters.

Figure 4 shows the six most stable isomeric structures for $(V_2O_5)_N^+$ (N = 2−6) clusters, denoted as $\mathbf{V_{2N}^+\_1}$−**6**. For $V_{12}O_{30}^+$ we obtained three more structures ($\mathbf{V_{12}^+\_7-9}$), shown in Supporting Information Figure S3, with relative energies less than 0.2 eV, which is the typical accuracy of B3LYP calculations. Our results indicate that $(V_2O_5)_N^+$ clusters prefer doublet state (with one unpaired electron), and they can be classified into two types according to the unpaired spin density (UPSD) distribution on them.

dx.doi.org/10.1021/jp5059403 | J. Phys. Chem. C 2014, 118, 24062−24071

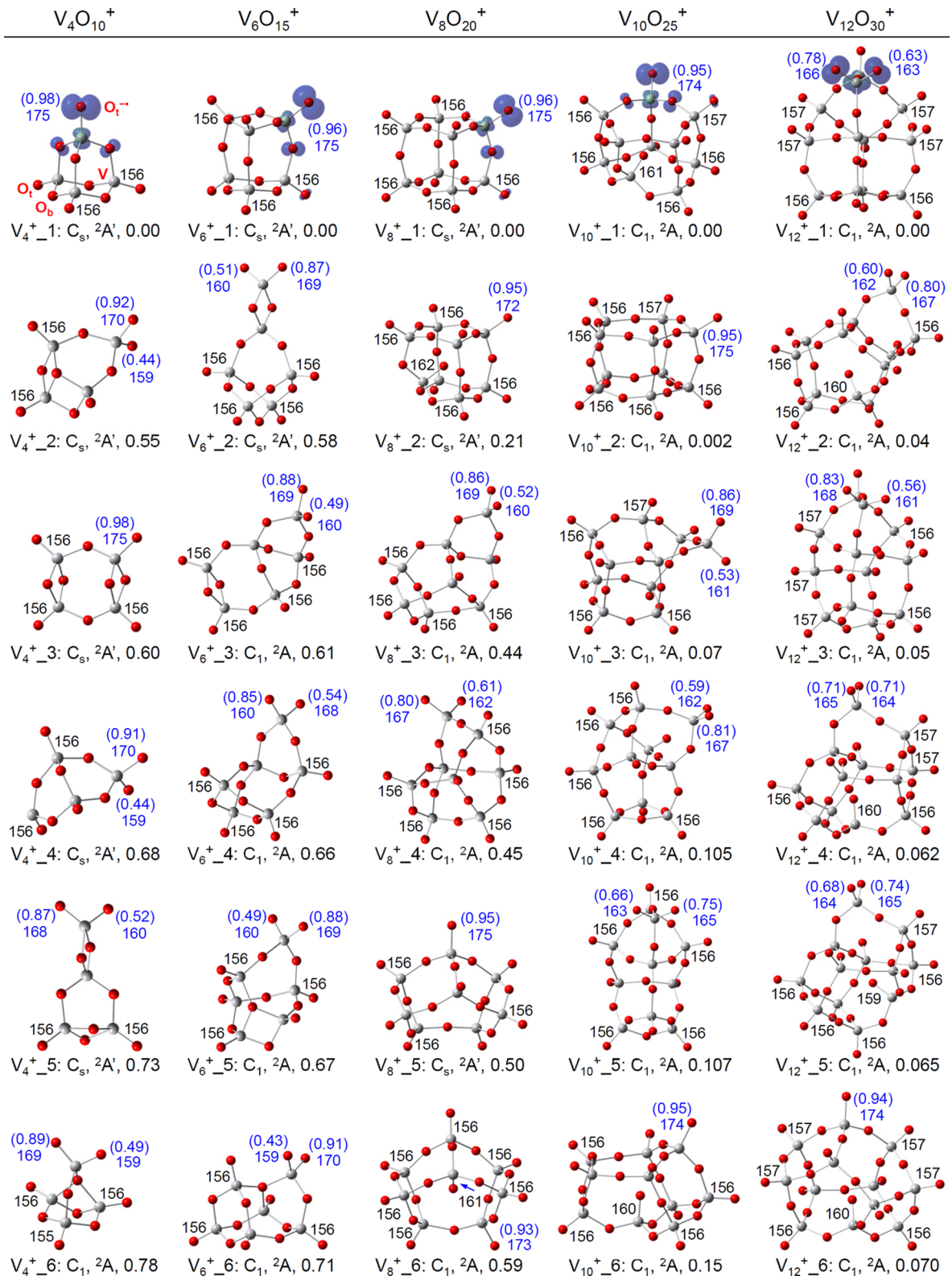

Figure 4. DFT optimized six most stable isomeric structures for each of the cationic $(V_2O_5)_N^+$ ($N = 2–6$) clusters. The symmetry, electronic state, and relative energy (eV) are listed below each structure. Some bond lengths of V−O_t are given in picometers. Mulliken spin density values (μ_B) over oxygen atoms are listed in parentheses, and profiles of the spin density distribution are plotted for the most stable clusters.

In the first type of structure such as **V_4^+_1**, the UPSD is mainly distributed on a 2p orbital of an O_t atom with a Mulliken value of about 1 μ_B, close to the UPSD value of the free O^- anion. This type of O_t is oxygen-centered radical that can be denoted as $O_t^{\bullet-}$. The bond length of V−$O_t^{\bullet-}$ is about 175 pm, which is much longer than those of V−O_t double bonds (about 156 pm, see Figures 3 and 4 for the bond lengths) and close to those of V−O_b single bonds (about 170−190 pm). Structures containing $O_t^{\bullet-}$

dx.doi.org/10.1021/jp5059403 | J. Phys. Chem. C 2014, 118, 24062−24071

are denoted as $O_t^{\bullet-}$-type structure, as in the cage-like polyhedron structures for the most stable isomers of $(V_2O_5)_N^+$ (N = 2−5) and the low-lying isomer $\mathbf{V_{12}^+\_6}$ (0.07 eV), as well as some nonpolyhedron structures such as $\mathbf{V_4^+\_3}$.

The second one is the $V(O_t)_2^{\bullet-}$-type structure (such as $\mathbf{V_{12}^+\_1}$), in which the UPSD is delocalized on two O_t atoms bonded to the same V atom, and the total spin density on the two O_t atoms is about 1.4 μ_B (about −0.4 μ_B on the V atom). In $V(O_t)_2^{\bullet-}$-type structures there often exists a V atom bonded with four O_b atoms (denoted as $V(O_b)_4$), such as in the five most stable isomers of $V_{12}O_{30}^+$ (i.e., $\mathbf{V_{12}^+\_1}$−$\mathbf{5}$) and some low-lying isomers of smaller clusters such as $\mathbf{V_4^+\_5}$, $\mathbf{V_6^+\_2}$, $\mathbf{V_8^+\_3}$, and $\mathbf{V_{10}^+\_3}$ with relative energy 0.73, 0.58, 0.44, 0.07 eV with respect to the most stable $O_t^{\bullet-}$-type structures. It is clear that $O_t^{\bullet-}$-type structures are preferred for relatively smaller clusters while $V(O_t)_2^{\bullet-}$-type ones are preferable for larger ones. The energy difference between two types of structures of large clusters is actually very small, less than 0.1 eV for both $(V_2O_5)_5^+$ and $(V_2O_5)_6^+$. $V(O_t)_2^{\bullet-}$-type structures can be viewed as a distortion from $O_t^{\bullet-}$-type ones by forming a new V−O bond and breaking an old one (see Supporting Information Figure S4 for an illustration). Some $V(O_t)_2^{\bullet-}$-type structures do not have a $V(O_b)_4$ moiety, but with a three-fold coordinated V, denoted as V(3), as in $\mathbf{V_4^+\_4}$, or a three-fold coordinated O, denoted as O(3), as in $\mathbf{V_4^+\_2}$, $\mathbf{V_4^+\_6}$, and $\mathbf{V_6^+\_5}$. These $V(O_t)_2^{\bullet-}$-type structures are all with high relative energies (higher than 0.5 eV with respect to the most stable polyhedron structures, and also higher than other $V(O_t)_2^{\bullet-}$-type structures without V(3) and O(3) for $N \geq 3$), so we speculate that $V(O_t)_2^{\bullet-}$-type structures are commonly accompanied by $V(O_b)_4$ moiety in large clusters.

Note that the most and metastable structures of $V_8O_{20}^+$ actually adopt the same polyhedron structure. The only difference is that in $\mathbf{V_8^+\_1}$ all the O_t atoms are outside the polyhedron (denoted as OutP structure), while in $\mathbf{V_8^+\_2}$ there is one O_t atom inside the polyhedron (InP). InP structure is preferred for larger clusters because the cavity inside the polyhedron of large clusters may be sufficiently large so that the repulsions between the inside O_t and the neighboring O_b atoms could be small. The relative energies of InP with respect to OutP for $(V_2O_5)_N^+$ clusters are +0.21, −0.002, and −0.09 eV for N = 4−6, respectively ($\mathbf{V_8^+\_2}$ vs $\mathbf{V_8^+\_1}$, $\mathbf{V_{10}^+\_1}$ vs $\mathbf{V_{10}^+\_2}$, and $\mathbf{V_{12}^+\_6}$ vs $\mathbf{V_{12}^+\_7}$). Similarly, neutral V_8O_{20} takes OutP as the most stable structure while $V_{12}O_{30}$ takes InP. For N < 4 clusters, InP structures are not stable or with high relative energies, such as InP of V_6O_{15} (**V6_4** in Supporting Information Figure S2) having relative energy as high as 1.27 eV. What is more, as distortions of polyhedron structures, some $V(O_t)_2^{\bullet-}$-type structures also have a large cavity, and one O_t atom can also be inside it. For example, all O_t atoms are out of the cavity in $\mathbf{V_{12}^+\_1}$, and if we move one O_t atom into the cavity and optimize the structure, we may get $\mathbf{V_{12}^+\_4}$ (0.062 eV) or $\mathbf{V_{12}^+\_5}$ (0.065 eV), depending on the selected O_t atom. For simplicity, we also call this type of structure as InP.

For neutral and cationic $(V_2O_5)_N$ clusters with N = 2−4, we obtained only one isomeric structure with relative energy less than 0.2 eV for each cluster. For N = 5 and 6, we obtained several isomeric structures with the energy difference less than 0.2 eV. For the cations, there are three $O_t^{\bullet-}$-type and three $V(O_t)_2^{\bullet-}$-type structures for N = 5, and two $O_t^{\bullet-}$-type and seven $V(O_t)_2^{\bullet-}$-type structures for N = 6. All of them may be reliable candidates for the ground state of each cluster. In practical experiments, geometric structures of clusters are also affected by the generation method, growth patterns, temperature, and so on, and some low-lying isomers may coexist under certain experimental conditions especially for large clusters,[79] with the experimental findings contributed from several different isomers. For a firm determination of the ground state structures, further studies are needed to combine valuable information from global structure optimization, quantum chemical calculations at different levels, and experiments such as IRPD, CID, and PES.

4. DISCUSSION

4.1. Structural Properties of Stoichiometric Vanadium Oxide Clusters. Neutral stoichiometric $(V_2O_5)_N$ clusters are all with closed-shell electronic structure, and it is reasonable to expect that all (or at least most) of the V atoms take +5 valence state and O atoms take −2 valence state. Thus, there could be three types of structural units with one V and several O atoms as shown in Figure 5a, $V(O_b)_3O_t$, $V(O_b)_5$, and $VO_b(O_t)_2$, assuming

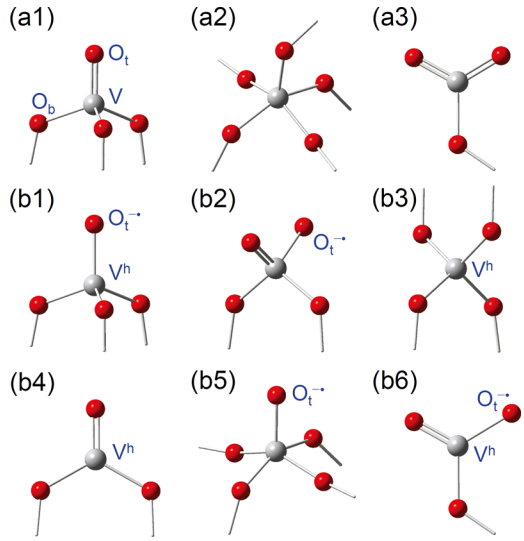

Figure 5. (a) Possible structural units in neutral and cationic $(V_2O_5)_N$ clusters. (b) Possible structural units only in cationic $(V_2O_5)_N$ clusters.

that only single or double bonds are between V and O atoms (no fractional bonds such as those with O(3)). Only the $V(O_b)_3O_t$ unit can be found in the low-lying structures (Supporting Information Figure S2, with relative energies less than 1 eV), which indicates that the $V(O_b)_3O_t$ unit (with four-coordinated V) is a more stable and geometrically more suitable building block than the others (with five- or three-coordinated V).[80] This further indicates that V atoms prefer four-fold coordination rather than three- or five-fold, and rationalizes the high stability of polyhedron structures for neutral $(V_2O_5)_N$ clusters that are constructed by 2N of $V(O_b)_3O_t$ unit. Structural units other than those in Figure 5a can only be found in some isomers with high relative energies (more than 1 eV), such as $V(O_b)_2(O_t)_2$ and O(3) in $\mathbf{V_4\_3}$ (1.72 eV).

In cationic $(V_2O_5)_N^+$ clusters, structural units may contain $O_t^{\bullet-}$ or V^h (the V^h atom makes 4 bonds with O atoms and a hole is assumed on it to preserve the +5 valence state). Thus, more possible structural units should be considered, as shown in Figure 5b. Interestingly, all these new units can be formed by breaking one V—O bond in the three structural units of neutral clusters with two possible pathways: $[V{=}O_t^{2-}] \rightarrow [V^h{-}O_t^{\bullet-}]^+ + e^-$, and $[V{-}O_b^{2-}{-}V] \rightarrow [V{-}O_t^{\bullet-} + V^h]^+ + e^-$. For example, breaking of one bond of the V=O double bond in $V(O_b)_3O_t$ (a1) results in the formation of $V^h(O_b)_3{-}O_t^{\bullet-}$ (b1), while

dx.doi.org/10.1021/jp5059403 | J. Phys. Chem. C 2014, 118, 24062−24071

Table 1. Data Related to the Reactivity of $(V_2O_5)_N^+$ (N = 2−6) Clusters with CH_4[a]

N	ΔH_{0K} (eV)	E_{LUMO} (eV)	VEA$^+$ (eV)	σ (μ_B)	E_b (eV)	Q_D (|e|)	Q_A (|e|)
2	−0.91	−11.9	10.23	0.906	0.26	0.208	0.106
3	−0.81	−11.4	9.89	0.805	0.17	0.164	0.089
4	−0.75	−11.1	9.67	0.743	0.15	0.141	0.077
5	−0.71 (−0.58)	−10.8 (−10.2)	9.46 (8.63)	0.715 (0.697)	0.11 (0.05)	0.128 (0.105)	0.076 (0.068)
6	−0.69 (−0.55)	−10.7 (−10.0)	9.36 (8.54)	0.709 (0.656)	0.10 (0.04)	0.118 (0.097)	0.070 (0.058)

[a]For $O_t^{\bullet-}$-type structures, data listed are the enthalpy of the HAA reaction (ΔH_{0K}); the energy of the lowest unoccupied molecular orbital (E_{LUMO}), the vertical electron affinity (VEA$^+$), and the unpaired spin density distributions (σ) on the $O_t^{\bullet-}$ atom of a cation; and the binding energy of CH_4 on cations (E_b) for [cation···CH_4] systems with the charge transfer: donated electrons from CH_4 (Q_D) and accepted electrons of $O_t^{\bullet-}$ (Q_A). Data for $V(O_t)_2^{\bullet-}$-type structures are listed in parentheses.

breaking of one V—O single bond or one O— dangling bond (actually an O—V bond with the V atom in another structural unit) leads to $V^h(O_b)_2O_t$ (b4) or $V(O_b)_2O_tO_t^{\bullet-}$ (b2), respectively. Theoretically, structures of $(V_2O_5)_N^+$ may be constructed by various combinations of these units: (2N − 1)a + b1/b6 (with both V^h and $O_t^{\bullet-}$), or (2N − 2)a + b3/b4 (with V^h only) + b2/b5 (with $O_t^{\bullet-}$ only). Fortunately, according to our obtained low-lying structures of neutral and cationic clusters, it is obvious that V atoms prefer four-fold coordination in the stoichiometric $(V_2O_5)_N$ and $(V_2O_5)_N^+$ clusters ($N \geq 2$). If we eliminate the units with three- or five-fold coordinated V, four types of units will be left as $V(O_b)_3O_t$ (a1), $V(O_b)_3O_t^{\bullet-}$ (b1), $V(O_b)_2O_tO_t^{\bullet-}$ (b2), and $V^h(O_b)_4$ (b3). Thus, there will be only two possible combinations of structural units: (2N − 1)a1 + b1 and (2N − 2)a1 + b2 + b3. The first combination results in the $O_t^{\bullet-}$-type structures, while the second one leads to the $V(O_t)_2^{\bullet-}$-type structures. Note that the $V(O_b)_2O_tO_t^{\bullet-}$ (b2) unit needs geometric and electronic relaxation and the spin density is redistributed onto both O_t atoms when it is adopted in the $V(O_t)_2^{\bullet-}$-type structures.

Actually, polyhedron structures have been obtained in previous works for neutral $(V_2O_5)_N$ (N = 2−5, 8, 10, and 12)[70,80−82] and cationic $(V_2O_5)_{2-4}^+$[26,64,80,83] clusters. Here, by means of (1) topological analysis to test all possible polyhedron structures, (2) structural unit analysis to consider all proper structural units, and (3) GA global optimization to avoid biased searching, we demonstrate that polyhedron structures, with additional InP structures being considered, are the ground state of neutral $(V_2O_5)_N$ and also candidates of the ground state of $(V_2O_5)_N^+$ (N = 2−6); what is more, we suggest that $V(O_t)_2^{\bullet-}$-type structures are also reliable candidates for the ground state for large cations (N = 5 and 6 in our calculations). Note that the $V(O_t)_2^{\bullet-}$ unit was previously found in cationic $V_2O_5^+$ (with a V(3) atom but no $V(O_b)_4$ moiety),[83−85] and it also widely exists in anionic $(V_2O_5)_NO^-$ clusters.[80] But $O_t^{\bullet-}$-type polyhedron structures are the most stable for all the $(V_2O_5)_N^+$ (N = 2−5) clusters, and the $V(O_t)_2^{\bullet-}$-type structures with $V(O_b)_4$ moiety are more stable than the polyhedron structures until the cluster size reaches nanosize, as for $(V_2O_5)_6^+$, which demonstrates the importance of studying large clusters for achieving unbiased conclusions.

In previous studies of $(V_2O_5)_{2-4}^+$ and many other subnanosized oxide cluster cations on which HAA reactions from CH_4 may take place, the UPSD was suggested on one O_t atom to form an $O_t^{\bullet-}$, and this type of oxygen-centered radical was suggested as the active site for C−H activation.[16,17,45,46] Here we suggest a new type of structure for $N \geq 5$ clusters, $V(O_t)_2^{\bullet-}$-type structure with a $V(O_b)_4$ moiety, in which the UPSD is distributed on two O_t atoms. Note that $V_2O_5^+$ with similar UPSD distribution like that in $V(O_t)_2^{\bullet-}$-type structures also have high reactivity toward CH_4,[27] so both $O_t^{\bullet-}$- and $V(O_t)_2^{\bullet-}$-type structures of $(V_2O_5)_N^+$ clusters can be used to rationalize their high reactivity found in the experiment with cluster sizes up to nanometers.

4.2. Interpretation of the Relative Reactivity. To study the relationship between the cluster reactivity in HAA with cluster size (N), various energetic and electronic properties have been studied for all ground state candidates of $(V_2O_5)_N^+$ (N = 2−6). For N = 5 and 6 clusters, similar properties are found for the isomers with the same $O_t^{\bullet-}$- or $V(O_t)_2^{\bullet-}$-type structures, so we list only the data for the most stable one of each type in Table 1 (i.e., $\mathbf{V_{10}}^+$**_1** and $\mathbf{V_{10}}^+$**_3** for N = 5, and $\mathbf{V_{12}}^+$**_1** and $\mathbf{V_{12}}^+$**_6** for N = 6). For different types of structures, the geometric and electronic structures of the active centers are quite different, so the reaction mechanisms of CH_4 on the two types of structures could be largely different from each other. We will discuss the properties of $O_t^{\bullet-}$-type structures at first.

Thermodynamic properties of the HAA reactions (eq 1) on $O_t^{\bullet-}$-type structures were calculated and the enthalpies of reactions (ΔH_{0K}) are all negative, indicates that HAA reactions on these clusters are all exothermal and thus favorable thermodynamically. The absolute values of ΔH_{0K} are found to decrease as N increases, which correlates well with the decrease of reactivity found in experiments.

HAA involves the transfer of one electron and one proton to the reacting clusters (H = e^- + proton$^+$). The electron is partially transferred from CH_4 to cluster cations in the initial stage of CH_4 activation, and electron transfer plays a key role in HAA.[42] To illustrate this issue clearly, model systems [cation···CH_4] were studied. In the calculations, the $O_t^{\bullet-}$···H distance is fixed at 2.0 Å, and the angle $O_t^{\bullet-}$···H−C is fixed at 170° while all the other geometric parameters are relaxed. The binding energy (E_b) is defined as $E_b = E(\text{cation}) + E(CH_4) - E(\text{cation}\cdots CH_4)$, where E is the total electronic energy without zero-point vibrational energy correction. Small cations with more concentrated charge distributions may cause larger polarization of the CH_4 molecule, leading to larger binding energies of CH_4 on them. Electron transfer from CH_4 (the donor) to the cations (the acceptors) is found for these systems, and the transferred electrons on the cations are mainly distributed on the $O_t^{\bullet-}$ atom. In Table 1, we list the values of electron transfer from natural population analysis (NPA), which are close to the values from Mulliken population. It is clear that fewer electrons are transferred as the cluster size increases, which correlates well with the reduced reactivity of large clusters.

Thus, the ability of a cluster to obtain an electron may highly influence its reactivity for HAA. Various properties of a cluster may reflect the ability to capture an electron. In Table 1 we list two of them: the energy of the lowest unoccupied molecular orbital (E_{LUMO}) and the vertical electron affinity of a cation

dx.doi.org/10.1021/jp5059403 | J. Phys. Chem. C 2014, 118, 24062−24071

(VEA^+), defined as the energy difference (without zero-point vibrational energy correction) between the cationic and neutral clusters with the equilibrium geometries of the cation (note that VEA^+ is different from the generally used vertical ionization potentials that are calculated with the equilibrium geometries of the neutral clusters). Cations with lower E_{LUMO} and higher VEA^+ are expected to be more likely to obtain an electron. Thus, the increase of E_{LUMO} and decrease of VEA^+ for $O_t^{\bullet-}$-type structures indicate that the clusters are less facile to obtain an electron as the cluster size increases, which may have a close relationship with the decrease of reactivity. The local electrostatic potentials (Supporting Information Figure S5) around the reaction center ($O_t^{\bullet-}$) for $O_t^{\bullet-}$-type structures are less positive for larger clusters thus providing less driving force for pulling electrons to the cluster cations. Electrostatic potential can be equivalent to effective charge distribution over the cluster. It is apparent that the net positive charge (+1 |e|) of a cation will be distributed to more atoms due to Coulomb repulsion as the cluster size increases, resulting in the less positive charge distribution around the reaction center. In a conclusion, various properties support that larger clusters have lower ability to capture an electron (electron effect), which leads to the lower reactivity of larger clusters.

It has been demonstrated that the localization versus delocalization of UPSD is a very important issue in the C−H activation by $O_t^{\bullet-}$-containing clusters.[17,46] Highly localized UPSD on the $O_t^{\bullet-}$ atom leads to high reactivity in HAA. In Figure 4 we have provided the Mulliken UPSD values on the $O_t^{\bullet-}$ atoms, which are qualitatively reasonable because the decrease of UPSD values is consistent with the reduced reactivity as N increases. However, the UPSD values are all very close to 1, which may hide the difference among clusters of different size. It is well-known that the calculated distribution of UPSD can be largely influenced by the computational methods, such as the Hartree-Fock component (HFC) in the B3LYP functional.[86,87] More HFC leads to higher localization of UPSD and vice versa. The HFC in B3LYP (20%) may be too high leading to high localization of UPSD for all the studied clusters. Test calculations by pure DFT functional BLYP (i.e., B3LYP with zero HFC) showed that UPSD of $V_4O_{10}^+$ is totally delocalized on four O_t atoms, which is not consistent with the high reactivity of $V_4O_{10}^+$ toward CH_4. This indicates that HFC cannot be too low either. We have tested several values for HFC, and in Table 1 we list the results obtained with HFC as 10%, just half of that in the original B3LYP functional. The UPSD values (σ) from Mulliken and NPA are very similar (differences are less than 0.004 μ_B), and in Table 1 we list only the Mulliken values. The numbers of σ are not necessarily rigorous, but a clear trend may be concluded that the σ values decrease by as large as 22% from N = 2 to 6. So the spin effect is another important reason for the reduction of reactivity as cluster size increases.

As for $V(O_t)_2^{\bullet-}$-type structures of $V_{10}O_{25}^+$ and $V_{12}O_{30}^+$, similar analysis is also performed (Table 1). In these analyses, one O_t atom in the $V(O_t)_2^{\bullet-}$ moiety with the bigger unpaired spin density, denoted as $O_t^{f\bullet-}$, acts as $O_t^{\bullet-}$ in $O_t^{\bullet-}$-type structures. That is, the H atom bonds to $O_t^{f\bullet-}$ in HAA, the CH_4 interacts with $O_t^{f\bullet-}$ ($O_t^{f\bullet-}\cdots H$ is 2.0 Å), and σ and Q_A are the spin and accepted electrons on $O_t^{f\bullet-}$. HAA reactions on $V(O_t)_2^{\bullet-}$-type structures are also exothermal, and N = 5 cluster releases more heat than the N = 6 cluster does, but less than $O_t^{\bullet-}$-type structures do. From the point of view of charge effect and spin effect, the difference between the data of N = 5 and 6 clusters all supports that the smaller cluster has higher reactivity, consistent with the experimental results. When compared with $O_t^{\bullet-}$-type structures, it is clear that $V(O_t)_2^{\bullet-}$-type ones are less willing to accept an electron according to the values of E_{LUMO}, VEA^+, and Q_D. This is quite apparent because for $V(O_t)_2^{\bullet-}$-type structures the corresponding neutral clusters are those with $V(O_b)_4$ and $V(O_b)_2(O_t)_2$ moieties, while $O_t^{\bullet-}$-type structures lead to stable polyhedron structures. The UPSD is delocalized on two O_t atoms in $V(O_t)_2^{\bullet-}$-type structures, and the UPSD value of each O_t atom is smaller than those of the $O_t^{\bullet-}$ atom in $O_t^{\bullet-}$-type structures. Additional energy is required to redistribute the UPSD onto the reacting O_t atom in the reactions with CH_4, as suggested for the anionic $V_2O_6^-$ cluster.[88,89] So, it is expected that, for a certain cluster, isomers with $V(O_t)_2^{\bullet-}$-type structures may have lower reactivity than those with $O_t^{\bullet-}$-type structures, from both thermodynamics and electronic structures. $V(O_t)_2^{\bullet-}$-type structures are more likely to appear in large clusters, which may be the third factor (structural effect) for the lower reactivity for the large clusters found in experiments.

4.3. Comparison with Bulk Oxide Materials. Gas-phase clusters are expected to reflect some characters (geometrical and electronic structures, reactivity, etc.) of the active sites and some nearby atoms in bulk materials. Especially, the active sites in large clusters may have similar substrate effect compared to those in bulk materials. So it is worthwhile to compare our results of clusters with those of bulk materials.

Structure of vanadium oxides in the crystalline state is well-documented in literature, which consists of VO_4 units as well as highly distorted VO_6 units.[90] The supported surface vanadia species are mainly present as isolated VO_4 units at low V concentration, and polymer or cluster species at high V concentration, while the exact structures are still unclear.[91] As for the clusters studied here, V atoms are all four-fold coordinated in the low-lying structures of both neutral and cationic $(V_2O_5)_N$ (N = 2−6) clusters, with only a few exceptions with high relative energies. Structures with $V(O_b)_4$ or inside O_t, that are found favorable in relatively large (N = 5 and 6) clusters, may have some relationship with the six-fold coordination of V in bulk materials, and studies on even larger clusters are needed to reach the high coordination of V atoms, which demonstrates that it is essential to study large clusters when cluster models are used to mimic the properties of bulk materials.

Electron holes localized around oxygen atoms have been found in both MgO and Li doped MgO,[92] which were suggested as the active sites for CH_4 activation.[92−96] The lattice O^{2-} with an electron hole can be viewed as $O^{\bullet-}$. For vanadia catalysts,[55] the pair of V^{4+} and $O^{\bullet-}$ was claimed to be an active center of CH_4 activation, and it can be generated by a charge transfer reaction $V^{5+} + O^{2-} = V^{4+} + O^-$, induced by light or elevated temperature. The presence of traces of V^{4+} in calcined vanadia catalyst at ambient and elevated temperature has been confirmed in some experiments.

It is clear that the $O^{\bullet-}$ in bulk catalysts is comparable to the oxygen-centered radicals in the oxide cluster cations. By studying the structure evolution of clusters up to nanosize, we suggest that not only the $O_t^{\bullet-}$-type but also the $V(O_t)_2^{\bullet-}$-type structures may serve as an active center in the supported vanadia species. In previous discussion, we assume that all V atoms in cations are still with +5 valence state, and V^h is viewed as $V^{4+} + h^+$. From the other point of view, since the highest occupied molecular orbitals (HOMO) of neutral $(V_2O_5)_N$ clusters (N = 2−6) are all localized on oxygen atoms, it is also reasonable to assume that the hole is near the $O_t^{\bullet-}$ site in the cations, and V^h is actually V^{4+}. Whatever picture is taken, the hole and the $O_t^{\bullet-}$ are close to each other in

dx.doi.org/10.1021/jp5059403 | J. Phys. Chem. C 2014, 118, 24062−24071

the $O_t^{\bullet-}$-type structures, in the same structural unit $V(O_b)_3O_t^{\bullet-}$, (Figure 5, b1) and it is possible for them to accept an electron to become stable unit $V(O_b)_3O_t$ (a1). So this type of active site in the catalysts is expected to be very unstable and easy to deactivate. On the other hand, in clusters with $V(O_t)_2^{\bullet-}$-type structures, the V^h or V^{4+} is in a $V(O_b)_4$ unit (b3) while the $O_t^{\bullet-}$ is in the $V(O_b)_2O_tO_t^{\bullet-}$ unit (b2). The two structural units may be separated by an O_b atom, as in $\mathbf{V_{12}^+\_1-5}$ isomers, or be separated even further with a little energy rise, as in $\mathbf{V_{12}^+\_9}$ (0.18 eV). Thus, it may happen in bulk materials that the formation of a V^h or V^{4+} moiety at one site results in an active site $V(O_t)_2^{\bullet-}$ far away. What is more, $V(O_t)_2^{\bullet-}$-type structures are not so able to accept an electron as $O_t^{\bullet-}$-type structures are. According to the theoretical calculation results on model clusters, $V(O_t)_2^{\bullet-}$-type structures have lower relative energies with respect to $O_t^{\bullet-}$-type ones for large clusters ($V_{12}O_{30}^+$), and they are not so able to accept an electron as $O_t^{\bullet-}$-type structures are. So it is expected that active sites with $V(O_t)_2^{\bullet-}$-type structures may be more stable (therefore higher concentration) on the surface than those with $O_t^{\bullet-}$-type structures do, and thus play a more important role in the catalytic reactions.

5. CONCLUSIONS

Vanadium oxide cluster cations have been prepared and reacted with CH_4 in a fast-flow reactor. Hydrogen atom abstraction (HAA) reactions were identified over stoichiometric cluster cations $(V_2O_5)_N^+$ ($N = 2-11$). The most stable structures of the clusters for $N = 2-6$ have been obtained by DFT calculations, and oxygen-centered radicals are found in all of these reactive clusters, which demonstrates their high reactivity toward CH_4. Two types of oxygen-centered radicals have been found on the nanosized clusters, leading to two types of geometric structures: $O_t^{\bullet-}$-type and $V(O_t)_2^{\bullet-}$-type. The newly found $V(O_t)_2^{\bullet-}$-type structures preferred for large clusters are suggested to be more stable on catalytic surfaces and play a more important role in catalytic reactions, as compared to the commonly known $O_t^{\bullet-}$-type structures. Large clusters have relatively lower reactivity than small clusters do, and the size-dependent reactivity is rationalized by the charge, spin, and structural effects. This work is among the first reports that HAA from CH_4 can take place on *nanosized* oxide clusters, which makes a bridge between small reactive species and inert condensed phase materials for CH_4 activation under low temperature, and may shed light on the rational design of (nano-) catalysts for practical methane conversions.

■ ASSOCIATED CONTENT

Supporting Information

Complete mass spectra for reactions of $V_xO_y^+$ with CH_4 and CD_4, low-lying isomeric structures for neutral $(V_2O_5)_N$ ($N = 2-6$) and $V_{12}O_{30}^+$, illustration of distortion from $O_t^{\bullet-}$-type to $V(O_t)_2^{\bullet-}$-type structures, and electrostatic potentials for the most stable $O_t^{\bullet-}$-type structures of $(V_2O_5)_N^+$ ($N = 2-6$). This material is available free of charge via the Internet at http://pubs.acs.org.

■ AUTHOR INFORMATION

Corresponding Authors

*E-mail: dingxl@ncepu.edu.cn.
*E-mail: chemzyx@iccas.ac.cn.

Notes

The authors declare no competing financial interest.

■ ACKNOWLEDGMENTS

This work is supported by CAS Knowledge Innovation Program (KJCX2-EW-H01), the National Natural Science Foundation of China (21173233 and 21203208), the Foundation of the ICCAS (CMS-PY-201202), the Major Research Plan of China (2011CB932302 and 2013CB834603), and the Fundamental Research Funds for the Central Universities (13ZD24, 2014ZZD10, 12ZP11, and 13TD03). We gratefully acknowledge the use of HPC cluster at School of Mathematics and Physics in NCEPU.

■ REFERENCES

(1) Crabtree, R. H. Aspects of Methane Chemistry. *Chem. Rev.* **1995**, *95*, 987−1007.
(2) Lunsford, J. H. Catalytic Conversion of Methane to More Useful Chemicals and Fuels: A Challenge for the 21st Century. *Catal. Today* **2000**, *63*, 165−174.
(3) Holmen, A. Direct Conversion of Methane to Fuels and Chemicals. *Catal. Today* **2009**, *142*, 2−8.
(4) Balcells, D.; Clot, E.; Eisenstein, O. C-H Bond Activation in Transition Metal Species from a Computational Perspective. *Chem. Rev.* **2010**, *110*, 749−823.
(5) Lai, W. Z.; Li, C. S.; Chen, H.; Shaik, S. Hydrogen-Abstraction Reactivity Patterns from A to Y: The Valence Bond Way. *Angew. Chem., Int. Ed.* **2012**, *51*, 5556−5578.
(6) Zhu, Q.; Wegener, S. L.; Xie, C.; Uche, O.; Neurock, M.; Marks, T. J. Sulfur as a Selective 'Soft' Oxidant for Catalytic Methane Conversion Probed by Experiment and Theory. *Nat. Chem.* **2013**, *5*, 104−109.
(7) Keil, F. J. Methane Activation: Oxidation Goes Soft. *Nat. Chem.* **2013**, *5*, 91−92.
(8) Enger, B. C.; Lødeng, R.; Holmen, A. A Review of Catalytic Partial Oxidation of Methane to Synthesis Gas with Emphasis on Reaction Mechanisms over Transition Metal Catalysts. *Appl. Catal., A* **2008**, *346*, 1−27.
(9) Lunsford, J. H. The Catalytic Oxidative Coupling of Methane. *Angew. Chem., Int. Ed.* **1995**, *34*, 970−980.
(10) Fokin, A. A.; Schreiner, P. R. Metal-Free, Selective Alkane Functionalizations. *Adv. Synth. Catal.* **2003**, *345*, 1035−1052.
(11) Lersch, M.; Tilset, M. Mechanistic Aspects of C-H Activation by Pt Complexes. *Chem. Rev.* **2005**, *105*, 2471−2526.
(12) Luo, L.; Tang, X.; Wang, W.; Wang, Y.; Sun, S.; Qi, F.; Huang, W. Methyl Radicals in Oxidative Coupling of Methane Directly Confirmed by Synchrotron VUV Photoionization Mass Spectroscopy. *Sci. Rep.* **2013**, *3*, 1625.
(13) Castleman, A. W., Jr. Cluster Structure and Reactions: Gaining Insights into Catalytic Processes. *Catal. Lett.* **2011**, *141*, 1243−1253.
(14) Wang, G. J.; Zhou, M. F. Probing the Intermediates in the MO $+CH_4 \leftrightarrow M+CH_3OH$ Reactions by Matrix Isolation Infrared Spectroscopy. *Int. Rev. Phys. Chem.* **2008**, *27*, 1−25.
(15) Roithová, J.; Schröder, D. Selective Activation of Alkanes by Gas-Phase Metal Ions. *Chem. Rev.* **2010**, *110*, 1170−1211.
(16) Schwarz, H. Chemistry with Methane: Concepts Rather than Recipes. *Angew. Chem., Int. Ed.* **2011**, *50*, 10096−10115.
(17) Dietl, N.; Schlangen, M.; Schwarz, H. Thermal Hydrogen-Atom Transfer from Methane: The Role of Radicals and Spin States in Oxo-Cluster Chemistry. *Angew. Chem., Int. Ed.* **2012**, *51*, 5544−5555.
(18) Shayesteh, A.; Lavrov, V. V.; Koyanagi, G. K.; Bohme, D. K. Reactions of Atomic Cations with Methane: Gas Phase Room-Temperature Kinetics and Periodicities in Reactivity. *J. Phys. Chem. A* **2009**, *113*, 5602−5611.
(19) Lang, S. M.; Bernhardt, T. M.; Barnett, R. N.; Landman, U. Methane Activation and Catalytic Ethylene Formation on Free Au_2^+. *Angew. Chem., Int. Ed.* **2010**, *49*, 980−983.
(20) Schröder, D.; Schwarz, H. Gas-Phase Activation of Methane by Ligated Transition-Metal Cations. *Proc. Natl. Acad. Sci. U.S.A.* **2008**, *105*, 18114−18119.

(21) Irikura, K. K.; Beauchamp, J. L. Osmium Tetroxide and Its Fragment Ions in the Gas Phase: Reactivity with Hydrocarbons and Small Molecules. *J. Am. Chem. Soc.* **1989**, *111*, 75−85.
(22) Schröder, D.; Fiedler, A.; Hrusak, J.; Schwarz, H. Experimental and Theoretical-Studies toward a Characterization of Conceivable Intermediates Involved in the Gas-Phase Oxidation of Methane by Bare FeO^+. Generation of Four Distinguishable $[Fe, C, H_4, O]^+$ Isomers. *J. Am. Chem. Soc.* **1992**, *114*, 1215−1222.
(23) Ryan, M. F.; Fiedler, A.; Schröder, D.; Schwarz, H. Radical-Like Behavior of Manganese Oxide Cation in Its Gas-Phase Reactions with Dihydrogen and Alkanes. *J. Am. Chem. Soc.* **1995**, *117*, 2033−2040.
(24) Kretzschmar, I.; Fiedler, A.; Harvey, J. N.; Schröder, D.; Schwarz, H. Effects of Sequential Ligation of Molybdenum Cation by Chalcogenides on Electronic Structure and Gas-Phase Reactivity. *J. Phys. Chem. A* **1997**, *101*, 6252−6264.
(25) Harvey, J. N.; Diefenbach, M.; Schröder, D.; Schwarz, H. Oxidation Properties of the Early Transition-Metal Dioxide Cations MO_2^+ (M = Ti, V, Zr, Nb) in the Gas-Phase. *Int. J. Mass Spectrom.* **1999**, *182/183*, 85−97.
(26) Feyel, S.; Döbler, J.; Schröder, D.; Sauer, J.; Schwarz, H. Thermal Activation of Methane by Tetranuclear $V_4O_{10}^+$. *Angew. Chem., Int. Ed.* **2006**, *45*, 4681−4685.
(27) Zhao, Y.-X.; Wu, X.-N.; Wang, Z.-C.; He, S.-G.; Ding, X.-L. Hydrogen-Atom Abstraction from Methane by Stoichiometric Early Transition Metal Oxide Cluster Cations. *Chem. Commun.* **2010**, *46*, 1736−1738.
(28) Wu, X.-N.; Zhao, Y.-X.; Xue, W.; Wang, Z.-C.; He, S.-G.; Ding, X.-L. Active Sites of Stoichiometric Cerium Oxide Cations ($Ce_mO_{2m}^+$) Probed by Reactions with Carbon Monoxide and Small Hydrocarbon Molecules. *Phys. Chem. Chem. Phys.* **2010**, *12*, 3984−3997.
(29) Schröder, D.; Roithová, J. Low-Temperature Activation of Methane: It Also Works Without a Transition Metal. *Angew. Chem., Int. Ed.* **2006**, *45*, 5705−5708.
(30) Sierka, M.; Döbler, J.; Sauer, J.; Santambrogio, G.; Brümmer, M.; Wöste, L.; Janssens, E.; Meijer, G.; Asmis, K. R. Unexpected Structures of Aluminum Oxide Clusters in the Gas Phase. *Angew. Chem., Int. Ed.* **2007**, *46*, 3372−3375.
(31) Feyel, S.; Döbler, J.; Hoeckendorf, R.; Beyer, M. K.; Sauer, J.; Schwarz, H. Activation of Methane by Oligomeric $(Al_2O_3)_x^+$ (x = 3,4,5): The Role of Oxygen-Centered Radicals in Thermal Hydrogen-Atom Abstraction. *Angew. Chem., Int. Ed.* **2008**, *47*, 1946−1950.
(32) Božović, A.; Bohme, D. K. Activation of X-H and X-D Bonds (X = O, N, C) by Alkaline-Earth Metal Monoxide Cations: Experiment and Theory. *Phys. Chem. Chem. Phys.* **2009**, *11*, 5940−5951.
(33) Zhang, X.; Schwarz, H. Thermal Activation of Methane by Diatomic Metal Oxide Radical Cations: $PbO^{+\bullet}$ as One of the Missing Pieces. *ChemCatChem* **2010**, *2*, 1391−1394.
(34) Chen, K.; Wang, Z. C.; Schlangen, M.; Wu, Y. D.; Zhang, X. H.; Schwarz, H. Thermal Activation of Methane and Ethene by Bare $MO^{\bullet+}$ (M = Ge, Sn, and Pb): A Combined Theoretical/Experimental Study. *Chem.—Eur. J.* **2011**, *17*, 9619−9625.
(35) de Petris, G.; Troiani, A.; Rosi, M.; Angelini, G.; Ursini, O. Methane Activation by Metal-Free Radical Cations: Experimental Insight into the Reaction Intermediate. *Chem.—Eur. J.* **2009**, *15*, 4248−4252.
(36) Dietl, N.; Engeser, M.; Schwarz, H. Room-Temperature C-H Bond Activation of Methane by Bare $[P_4O_{10}]^{\bullet+}$. *Angew. Chem., Int. Ed.* **2009**, *48*, 4861−4863.
(37) Dietl, N.; Troiani, A.; Schlangen, M.; Ursini, O.; Angelini, G.; Apeloig, Y.; de Petris, G.; Schwarz, H. Mechanistic Aspects of Gas-Phase Hydrogen-Atom Transfer from Methane to $[CO]^{\bullet+}$ and $[SiO]^{\bullet+}$: Why Do They Differ? *Chem.—Eur. J.* **2013**, *19*, 6662−6669.
(38) Wang, Z.-C.; Wu, X.-N.; Zhao, Y.-X.; Ma, J.-B.; Ding, X.-L.; He, S.-G. Room-Temperature Methane Activation by a Bimetallic Oxide Cluster $AlVO_4^+$. *Chem. Phys. Lett.* **2010**, *489*, 25−29.
(39) Ding, X.-L.; Zhao, Y.-X.; Wu, X.-N.; Wang, Z.-C.; Ma, J.-B.; He, S.-G. Hydrogen-Atom Abstraction from Methane by Stoichiometric Vanadium-Silicon Heteronuclear Oxide Cluster Cations. *Chem.—Eur. J.* **2010**, *16*, 11463−11470.
(40) Dietl, N.; Hockendorf, R. F.; Schlangen, M.; Lerch, M.; Beyer, M. K.; Schwarz, H. Generation, Reactivity Towards Hydrocarbons, and Electronic Structure of Heteronuclear Vanadium Phosphorous Oxygen Cluster Ions. *Angew. Chem., Int. Ed.* **2011**, *50*, 1430−1434.
(41) Ma, J.-B.; Wu, X.-N.; Zhao, Y.-X.; Ding, X.-L.; He, S.-G. Methane Activation by $V_3PO_{10}^+$ and $V_4O_{10}^+$ Clusters: A Comparative Study. *Phys. Chem. Chem. Phys.* **2010**, *12*, 12223−12228.
(42) Li, Z.-Y.; Zhao, Y.-X.; Wu, X.-N.; Ding, X.-L.; He, S.-G. Methane Activation by Yttrium-Doped Vanadium Oxide Cluster Cations: Local Charge Effects. *Chem.—Eur. J.* **2011**, *17*, 11728−11733.
(43) Ma, J.-B.; Wang, Z.-C.; Schlangen, M.; He, S.-G.; Schwarz, H. Thermal Reactions of $YAlO_3^{+\bullet}$ With Methane: Increasing the Reactivity of $Y_2O_3^{+\bullet}$ and the Selectivity of $Al_2O_3^{+\bullet}$ by Doping. *Angew. Chem., Int. Ed.* **2012**, *51*, 5991−5994.
(44) Wu, X.-N.; Li, X.-N.; Ding, X.-L.; He, S.-G. Activation of Multiple C-H Bonds Promoted by Gold in $AuNbO_3^+$ Clusters. *Angew. Chem., Int. Ed.* **2013**, *52*, 2444−2448.
(45) Zhao, Y.-X.; Wu, X.-N.; Ma, J.-B.; He, S.-G.; Ding, X.-L. Characterization and Reactivity of Oxygen-Centred Radicals over Transition Metal Oxide Clusters. *Phys. Chem. Chem. Phys.* **2011**, *13*, 1925−1938.
(46) Ding, X.-L.; Wu, X.-N.; Zhao, Y.-X.; He, S.-G. C-H Bond Activation by Oxygen-Centered Radicals over Atomic Clusters. *Acc. Chem. Res.* **2012**, *45*, 382−390.
(47) Viggiano, A. A.; Morris, R. A.; Miller, T. M.; Friedman, J. F.; Menedez-Barreto, M.; Paulson, J. F.; Michels, H. H.; Hobbs, R. H.; Montgomery, J. A. Reaction on the $O^- + CH_4$ Potential Energy Surface: Dependence on Translational and Internal Energy and on Isotopic Composition, 93−1313 K. *J. Chem. Phys.* **1997**, *106*, 8455−8463.
(48) In this work, the diameter is estimated for a round ball with the mass density of the bulk materials. Densities for bulk Al_2O_3, Sc_2O_3, and V_2O_5 are 3.97, 3.86, and 3.35 g cm^{-3}, respectively, taken from the following handbook (ref 49).
(49) Lide, D. R. *CRC Handbook of Chemistry and Physics*, 84th ed.; CRC Press: Boca Raton, FL, 2003.
(50) Wu, X.-N.; Xu, B.; Meng, J.-H.; He, S.-G. C-H Bond Activation by Nanosized Scandium Oxide Clusters in Gas-Phase. *Int. J. Mass Spectrom.* **2012**, *310*, 57−64.
(51) Weckhuysen, B. M.; Keller, D. E. Chemistry, Spectroscopy and the Role of Supported Vanadium Oxides in Heterogeneous Catalysis. *Catal. Today* **2003**, *78*, 25−46.
(52) Amiridis, M. D.; Rekoske, J. E.; Dumesic, J. A.; Rudd, D. F.; Spencer, N. D.; Pereira, C. J. Simulation of Methane Partial Oxidation over Silica-Supported MoO_3 and V_2O_5. *AIChE J.* **1991**, *37*, 87−97.
(53) Banares, M. A.; Cardoso, J. H.; Hutchings, G. J.; Bueno, J. M. C.; Fierro, J. L. G. Selective Oxidation of Methane to Methanol and Formaldehyde over V_2O_5/SiO_2 Catalysts. Role of NO in the Gas Phase. *Catal. Lett.* **1998**, *56*, 149−153.
(54) Miao, S.; Ma, D.; Zhu, Q.; Zheng, H.; Jia, G.; Zhou, S.; Bao, X. On the Role of Vanadia Species for VO_x/SiO_2 in the Selective Oxidation of Methane. *J. Nat. Gas Chem.* **2005**, *14*, 77−87.
(55) Lojewska, J.; Zralka, B.; Makowski, W.; Dziembaj, R. Promoting Methane Partial Oxidation: Homogenous Additives Impact on Formaldehyde Yield on Vanadia Catalyst. *Catal. Today* **2005**, *101*, 73−80.
(56) Pirovano, C.; Schonborn, E.; Wohlrab, S.; Kalevaru, V. N.; Martin, A. On the Performance of Porous Silica Supported VO_x Catalysts in the Partial Oxidation of Methane. *Catal. Today* **2012**, *192*, 20−27.
(57) Xue, W.; Wang, Z.-C.; He, S.-G.; Xie, Y.; Bernstein, E. R. Experimental and Theoretical Study of the Reactions between Small Neutral Iron Oxide Clusters and Carbon Monoxide. *J. Am. Chem. Soc.* **2008**, *130*, 15879−15888.
(58) Wu, X.-N.; Ma, J.-B.; Xu, B.; Zhao, Y.-X.; Ding, X.-L.; He, S.-G. Collision-Induced Dissociation and Density Functional Theory Studies of CO Adsorption over Zirconium Oxide Cluster Ions: Oxidative and Nonoxidative Adsorption. *J. Phys. Chem. A* **2011**, *115*, 5238−5246.
(59) Lee, C. T.; Yang, W. T.; Parr, R. G. Development of the Colle-Salvetti Correlation-Energy Formula into a Functional of the Electron-Density. *Phys. Rev. B* **1988**, *37*, 785−789.

(60) Becke, A. D. Density-Functional Thermochemistry 3: The Role of Exact Exchange. *J. Chem. Phys.* **1993**, *98*, 5648−5652.
(61) Becke, A. D. Density-Functional Exchange-Energy Approximation with Correct Asymptotic-Behavior. *Phys. Rev. A* **1988**, *38*, 3098−3100.
(62) Frisch, M. J.; Trucks, G. W.; Schlegel, H. B.; Scuseria, G. E.; Robb, M. A.; Cheeseman, J. R.; Scalmani, G.; Barone, V.; Mennucci, B.; Petersson, G. A.; et al. *Gaussian 09, Revision A.01*; Gaussian, Inc.: Wallingford, CT, 2009.
(63) Asmis, K. R.; Wende, T.; Brummer, M.; Gause, O.; Santambrogio, G.; Stanca-Kaposta, E. C.; Dobler, J.; Niedziela, A.; Sauer, J. Structural Variability in Transition Metal Oxide Clusters: Gas Phase Vibrational Spectroscopy of $V_3O_{6-8}^+$. *Phys. Chem. Chem. Phys.* **2012**, *14*, 9377−9388.
(64) Asmis, K. R.; Sauer, J. Mass-Selective Vibrational Spectroscopy of Vanadium Oxide Cluster Ions. *Mass Spectrom. Rev.* **2007**, *26*, 542−562.
(65) Santambrogio, G.; Brümmer, M.; Wöste, L.; Döbler, J.; Sierka, M.; Sauer, J.; Meijer, G.; Asmis, K. R. Gas Phase Vibrational Spectroscopy of Mass-Selected Vanadium Oxide Anions. *Phys. Chem. Chem. Phys.* **2008**, *10*, 3992−4005.
(66) Fielicke, A.; Mitrić, R.; Meijer, G.; Bonačić-Koutecký, V.; von Helden, G. The Structures of Vanadium Oxide Cluster-Ethene Complexes. A Combined IR Multiple Photon Dissociation Spectroscopy and DFT Calculation Study. *J. Am. Chem. Soc.* **2003**, *125*, 15716−15717.
(67) Bell, R. C.; Zemski, K. A.; Justes, D. R.; Castleman, A. W., Jr. Formation, Structure and Bond Dissociation Thresholds of Gas-Phase Vanadium Oxide Cluster Ions. *J. Chem. Phys.* **2001**, *114*, 798−811.
(68) Koyanagi, G. K.; Bohme, D. K.; Kretzschmar, I.; Schröder, D.; Schwarz, H. Gas-Phase Chemistry of Bare V^+ Cation with Oxygen and Water at Room Temperature: Formation and Hydration of Vanadium Oxide Cations. *J. Phys. Chem. A* **2001**, *105*, 4259−4271.
(69) Zhang, X. H.; Schwarz, H. Generation of Gas-Phase Nanosized Vanadium Oxide Clusters from a Mononuclear Precursor by Solution Nucleation and Electrospray Ionization. *Chem.—Eur. J.* **2010**, *16*, 1163−1167.
(70) Zhai, H. J.; Dobler, J.; Sauer, J.; Wang, L. S. Probing the Electronic Structure of Early Transition-Metal Oxide Clusters: Polyhedral Cages of $(V_2O_5)_n^-$ (n = 2−4) and $(M_2O_5)_2^-$ (M = Nb, Ta). *J. Am. Chem. Soc.* **2007**, *129*, 13270−13276.
(71) Ding, X.-L.; Li, Z.-Y.; Meng, J.-H.; Zhao, Y.-X.; He, S.-G. Density-Functional Global Optimization of $(La_2O_3)_n$ Clusters. *J. Chem. Phys.* **2012**, *137*, 214311.
(72) Dunning, T. H., Jr.; Hay, P. J. *Modern Theoretical Chemistry*; Schaefer, H. F., III, Ed.; Plenum: New York, 1976; Vol. 3.
(73) Hay, P. J.; Wadt, W. R. Abinitio Effective Core Potentials for Molecular Calculations—Potentials for K to Au Including the Outermost Core Orbitals. *J. Chem. Phys.* **1985**, *82*, 299−310.
(74) Wadt, W. R.; Hay, P. J. Abinitio Effective Core Potentials for Molecular Calculations—Potentials for Main Group Elements Na to Bi. *J. Chem. Phys.* **1985**, *82*, 284−298.
(75) Schafer, A.; Huber, C.; Ahlrichs, R. Fully Optimized Contracted Gaussian-Basis Sets of Triple Zeta Valence Quality for Atoms Li to Kr. *J. Chem. Phys.* **1994**, *100*, 5829−5835.
(76) The diameters of $(V_2O_5)_N$, N = 6, 7, 10, 11 were calculated (see ref 48) to be 1.01, 1.06, 1.20, and 1.24 nm, respectively.
(77) Taking that the cluster beam velocity is about 1 km s^{-1}, the radius of CH_4 is 0.16 nm, and radii of $(V_2O_5)_N^+$ are estimated as round balls (see ref 48).
(78) Brinkmann, G.; Friedrichs, O. D.; Lisken, S.; Peeters, A.; Van Cleemput, N. CaGe—A Virtual Environment for Studying Some Special Classes of Plane Graphs—An Update. *MATCH Commun. Math. Comput. Chem.* **2010**, *63*, 533−552.
(79) Hakkinen, H.; Yoon, B.; Landman, U.; Li, X.; Zhai, H. J.; Wang, L. S. On the Electronic and Atomic Structures of Small Au_N^- (N=4−14) Clusters: A Photoelectron Spectroscopy and Density-Functional Study. *J. Phys. Chem. A* **2003**, *107*, 6168−6175.
(80) Ma, Y.-P.; Zhao, Y.-X.; Li, Z.-Y.; Ding, X.-L.; He, S.-G. Classification of $V_xO_y^q$ Clusters by Δ=2y+q-5x. *Chin. J. Chem. Phys.* **2011**, *24*, 586−596.
(81) Vyboishchikov, S. F.; Sauer, J. $(V_2O_5)_n$ Gas-Phase Clusters (n = 1−12) Compared to V_2O_5 Crystal: DFT Calculations. *J. Phys. Chem. A* **2001**, *105*, 8588−8598.
(82) Jakubikova, E.; Rappe, A. K.; Bernstein, E. R. Density Functional Theory Study of Small Vanadium Oxide Clusters. *J. Phys. Chem. A* **2007**, *111*, 12938−12943.
(83) Justes, D. R.; Mitrić, R.; Moore, N. A.; Bonačić-Koutecký, V.; Castleman, A. W., Jr. Theoretical and Experimental Consideration of the Reactions between $V_xO_y^+$ and Ethylene. *J. Am. Chem. Soc.* **2003**, *125*, 6289−6299.
(84) Calatayud, M.; Andres, J.; Beltran, A. A Systematic Density Functional Theory Study of $V_xO_y^+$ and V_xO_y (x = 2−4, y = 2−10) Systems. *J. Phys. Chem. A* **2001**, *105*, 9760−9775.
(85) Asmis, K. R.; Meijer, G.; Brümmer, M.; Kaposta, C.; Santambrogio, G.; Wöste, L.; Sauer, J. Gas Phase Infrared Spectroscopy of Mono- and Divanadium Oxide Cluster Cations. *J. Chem. Phys.* **2004**, *120*, 6461−6470.
(86) Asmis, K. R.; Santambrogio, G.; Brümmer, M.; Sauer, J. Polyhedral Vanadium Oxide Cages: Infrared Spectra of Cluster Anions and Size-Induced D Electron Localization. *Angew. Chem., Int. Ed.* **2005**, *44*, 3122−3125.
(87) Solans-Monfort, X.; Branchadell, V.; Sodupe, M.; Sierka, M.; Sauer, J. Electron Hole Formation in Acidic Zeolite Catalysts. *J. Chem. Phys.* **2004**, *121*, 6034−6041.
(88) Ma, J.-B.; Wu, X.-N.; Zhao, Y.-X.; He, S.-G.; Ding, X.-L. Experimental and Theoretical Studies of the Reactions between Vanadium Oxide Cluster Anions and Small Hydrocarbon Molecules. *Acta Phys.-Chim. Sin.* **2010**, *26*, 1761−1767.
(89) Zhao, Y.-X.; Wu, X.-N.; Ma, J.-B.; He, S.-G.; Ding, X.-L. Experimental and Theoretical Study of the Reactions between Vanadium-Silicon Heteronuclear Oxide Cluster Anions with N-Butane. *J. Phys. Chem. C* **2010**, *114*, 12271−12279.
(90) Wachs, I. E.; Briand, L. E.; Jehng, J. M.; Burcham, L.; Gao, X. T. Molecular Structure and Reactivity of the Group V Metal Oxides. *Catal. Today* **2000**, *57*, 323−330.
(91) Ding, X.-L.; Xue, W.; Ma, Y.-P.; Zhao, Y.-X.; Wu, X.-N.; He, S.-G. Theoretical Investigation of the Selective Oxidation of Methanol to Formaldehyde on Vanadium Oxide Species Supported on Silica: Umbrella Model. *J. Phys. Chem. C* **2010**, *114*, 3161−3169.
(92) Chiesa, M.; Giamello, E.; Che, M. EPR Characterization and Reactivity of Surface-Localized Inorganic Radicals and Radical Ions. *Chem. Rev.* **2010**, *110*, 1320−1347.
(93) Arndt, S.; Laugel, G.; Levchenko, S.; Horn, R.; Baerns, M.; Scheffler, M.; Schlögl, R.; Schomäcker, R. A Critical Assessment of Li/MgO-Based Catalysts for the Oxidative Coupling of Methane. *Catal. Rev.: Sci. Eng.* **2011**, *53*, 424−514.
(94) Liu, H. F.; Liu, R. S.; Liew, K. Y.; Johnson, R. E.; Lunsford, J. H. Partial Oxidation of Methane by Nitrous-Oxide over Molybdenum on Silica. *J. Am. Chem. Soc.* **1984**, *106*, 4117−4121.
(95) Launay, H.; Loridant, S.; Nguyen, D. L.; Volodin, A. M.; Dubois, J. L.; Millet, J. M. M. Vanadium Species in New Catalysts for the Selective Oxidation of Methane to Formaldehyde: Activation of the Catalytic Sites. *Catal. Today* **2007**, *128*, 176−182.
(96) Panov, G. I.; Dubkov, K. A.; Starokon, E. V. Active Oxygen in Selective Oxidation Catalysis. *Catal. Today* **2006**, *117*, 148−155.